

Theoretical model for analysis of elastic constants in orthotropic materials considering shear stress

Á. S. Alves^a, M. S. R. Miltão^b, E. S. Ferreira^c and J. A. Leyva Cruz^b

^a*Physics Laboratory on Campus, Department of Physics, State University of Feira de Santana, Avenida Transnordestina, s/n - Novo Horizonte, 44036-900, Feira de Santana, Bahia, Brazil.*

^b*Laboratory of Instrumentation in Physics, Department of Physics, State University of Feira de Santana, Avenida Transnordestina, s/n - Novo Horizonte, Feira de Santana, 44036-900, Bahia, Brazil.*

^c*Laboratory of Spectroscopy, Nanomaterials and Sensors, Department of Physics, State University of Feira de Santana, Avenida Transnordestina, s/n - Novo Horizonte, Feira de Santana, 44036-900, Bahia, Brazil.*

Received 29 November 2023; accepted 11 August 2024

Nowadays, a general theoretical model to describe the mechanical behavior of anisotropic or orthotropic materials is still an open challenge. In this study, we propose a new theoretical model to determine the elastic constants of these materials considering the shear components of the stress tensor. To analyze the consistency of new approach in biaxial stress state on thin films, we used the experimental data reported in the literature, based in the $\sin^2 \psi$ technique. Here we reported, the shear modulus value equal to $G_{xz} = 0.3$ GPa, for a polycrystalline Au thin film, was calculated, in addition to other elastic constants. Finally, we demonstrate that the new proposal theoretical model considering shear stress can be useful to determine elastic constants in orthotropic materials from experimentally measured data.

Keywords: Elastic constants; Young modulus; Poissons ratio; shear modulus.

DOI: <https://doi.org/10.31349/RevMexFis.70.061004>

1. Introduction

Nowadays, determining the values of the elastic constants are one of most important challenge in the materials physics area. For example, some studies have been standardized some materials as Au thin-films, to measurement relevant elastic parameters such, as Poisson's ratio, Young's and Shear modulus. These elastic constants are used to characterize and design new materials in physics and engineering area. In this field, there are a growing number of studies relating to the analysis of biaxial and triaxial stress in orthotropic materials [1–11].

Despite this growth there is still no complete theoretical model that explains all the elastic properties of these materials types. In several applications real loads can induce complex multiaxial fatigue problems. Furthermore, a general model for full elastic constants analyses in orthotropic materials are necessary. As discussed in the literature, the study of stress is of interest for a wide range of applications [12–15]. Thus, it is important the search of theoretical models that enable us the investigation of the stress-strain relation in a material, to determine its elastic constants.

As is well know, stresses in a material cannot be directly measured and to obtain the stress we need to measure, for example, the deformation. In a material the stresses originate from many sources and can be divided into three categories considering their length scale. Elastic constants measure the proportionality between strain and stress in a material, always that the strain is not so large as to violate Hook's law [16–19].

Experimentally, a elastic constant is determined by applying a strain to a crystal, measuring the energy versus strain,

and determining the elastic constant from the curvature of this function at zero strain. The values of strain are associated to a linear combination of elastic constants.

An important point to be emphasized is that the stress is strongly dependent on the material's anisotropy. Anisotropy in a material is known as the dependence of its crystalline properties in terms of its directions.

The preferential orientation inside a material is called the texture [20], that is an intrinsic characteristic of metals, ceramics, polymers, and rocks and it has a strong effect on the anisotropy of the physical properties of a material. The effect of texture on stress is a well-known and ongoing problem [21] and is still an open issue from the theoretical and experimental points of view [22–29]. In a recent work were determined the elastic constants for a material with orthotropic symmetry, neglecting the shear stress [1] using a novel model. In this study, we propose a new theoretical model to determine the elastic constants of the orthotropic materials considering the shear components of the stress tensor.

The following sections of the paper are organized as follows. Section 2 describes the basic theoretical expression for stress states considering orthotropic materials. In Sec. 3, the expression for a new theoretical model for triaxial and biaxial stress states for orthotropic materials, considering the shear stress, are shown. After that, the new theoretical model proposed, are evaluated for the biaxial stress state, for thin films. Finally, the conclusions are exposed.

2. Expressions for Stress States considering Orthotropic Materials

In the model is considered the constitutive relation between stress and strain, *i.e.*, the generalized Hooke's law. Taking into consideration the fact that from the experimental point of view the stress is usually measured by a diffraction technique, our model can be applied to diffraction techniques (X-rays and neutrons), because the experimental conditions are consistent with those assumed in the model, *i.e.*, (a) small deformations in comparison with the sample dimensions and (b) the stress involved is not sufficient to change the material volume. The first step was to determine the components of the orthotropic elasticity tensor, given by Eq. (17) of Ref. [1]. For this we use the elements of the orthotropic symmetry group with a phenomenological approach. As we saw, the characterization of the elastic behavior of an orthotropic

material is given by nine independent constants that in phenomenological terms are referred to as three longitudinal moduli of elasticity or Young's moduli (E_x, E_y, E_z), three transverse moduli of elasticity or shear moduli (G_{xy}, G_{yz}, G_{zx}) and three Poisson coefficients ($\nu_{xy}, \nu_{yz}, \nu_{zx}$).

Considering the Generalized Hooke's law

$$\sigma_{ij} = \Lambda_{ijkl} \varepsilon_{kl}, \quad (1)$$

the inverse is given by

$$\varepsilon_{kl} = \Lambda_{kl ij}^{-1} \sigma_{ij}, \quad (2)$$

where Λ_{ijkl} is the tensor of the elasticity and $\Lambda_{kl ij}^{-1}$ is the tensor of stiffness. In the Voigt space and using the stiffness tensor, the elastic behavior of an orthotropic material is represented as follows,

$$\begin{pmatrix} \varepsilon_{xx} \\ \varepsilon_{yy} \\ \varepsilon_{zz} \\ \varepsilon_{yz} \\ \varepsilon_{xz} \\ \varepsilon_{xy} \end{pmatrix} = \begin{pmatrix} \frac{1}{E_x} & -\frac{\nu_{yx}}{E_y} & -\frac{\nu_{zx}}{E_z} & 0 & 0 & 0 \\ -\frac{\nu_{xy}}{E_x} & \frac{1}{E_y} & -\frac{\nu_{zy}}{E_z} & 0 & 0 & 0 \\ -\frac{\nu_{xz}}{E_x} & -\frac{\nu_{yz}}{E_y} & \frac{1}{E_z} & 0 & 0 & 0 \\ 0 & 0 & 0 & \frac{1}{2G_{yz}} & 0 & 0 \\ 0 & 0 & 0 & 0 & \frac{1}{2G_{xz}} & 0 \\ 0 & 0 & 0 & 0 & 0 & \frac{1}{2G_{xy}} \end{pmatrix} \begin{pmatrix} \sigma_{xx} \\ \sigma_{yy} \\ \sigma_{zz} \\ \tau_{yz} \\ \tau_{xz} \\ \tau_{xy} \end{pmatrix}, \quad (3)$$

To consider a measurement we need to use an orthonormal coordinate system coincident with the axes of the sample P_i axis and a laboratory coordinate system L_i . So we use a transformation of the coordinates between the two reference systems and the relationship between the strain tensors in the two coordinate systems is given by,

$$\varepsilon'_{ij} = w_{ik} \varepsilon_{kl} w_{jl}^T, \quad (4)$$

where ε_{ij} is the strain tensor in the system P_i , ε'_{ij} is the strain tensor in the laboratory system L_i , and w is the matrix giving the coordinate transformation between P_i and L_i , obtained from.

$$w_{ik} = a_{ij} a_{jk}, \quad (5)$$

where

$$a_{ij} = \begin{pmatrix} \cos \psi & 0 & -\sin \psi \\ 0 & 1 & 0 \\ \sin \psi & 0 & \cos \psi \end{pmatrix},$$

and

$$a_{jk} = \begin{pmatrix} \cos \phi & \sin \phi & 0 \\ -\sin \phi & \cos \phi & 0 \\ 0 & 0 & 1 \end{pmatrix},$$

here the angles ψ and ϕ are, respectively, the Euler angles, referred to rotations of a rigid body in the xz and xy planes, for more details see Fig. 1 of the Ref. [1]. In the Voigt space we have for the matrix w_{ik} that give the coordinate transformation:

$$M_w = F \underline{w} F^{-1}, \quad (6)$$

where the matrix F and \underline{w} are the same found in Ref. [31]. So, we have to M_w ,

Re-writing the Eq. (4) in Voigt space, we find the following relations

$$(7) \quad \varepsilon' = M_w \varepsilon, \quad (8)$$

where ε is the six-dimensional strain vector in the system P_i , ε' is the six-dimensional strain vector in the laboratory system L_i , and M_w is the matrix giving the coordinate transformation between P_i and L_i , obtained from (6). So, the expression for the strain vector in both systems, considering the L_3 direction is given by,

$$\begin{aligned} \varepsilon_{z'z'} &= \cos^2 \phi \sin^2 \psi \varepsilon_{xx} + \sin 2\phi \sin^2 \psi \varepsilon_{xy} \\ &\quad + \cos \phi \sin 2\psi \varepsilon_{xz} + \sin^2 \phi \sin^2 \psi \varepsilon_{yy} \\ &\quad + \sin 2\psi \sin \phi \varepsilon_{yz} + \cos^2 \psi \varepsilon_{zz}, \\ \varepsilon_{x'x'} &= \varepsilon_{y'y'} = 0, \\ \varepsilon_{y'z'} &= \varepsilon_{z'x'} = \varepsilon_{x'y'} = 0. \end{aligned} \quad (9)$$

To carry out the phenomenological approach, we choose one direction as the direction of the experimental measurement (L_3 direction) and assume that the shear stresses are negligible, according with Ref. [1]. The strain and stress tensors are always related to the axis in the phenomenological approach. Therefore, we will study the states of the triaxial stress when there are tensions in the x , y , and z directions and the states of the biaxial stress when there are tensions in the x and y directions.

3. New theoretical model for analysis of biaxial and triaxial stress in orthotropic materials considering the shear stress

A state equation of triaxial stresses is obtained substituting the theoretical Eq. (3) in Eq. (9), representing the experimental situation, and after appropriate manipulations, we arrive the following result, which relates strain with triaxial stress for orthotropic materials:

$$\begin{aligned} \varepsilon_{z'z'} &= \sin^2 \psi \left\{ \frac{\sigma_{xx}}{E_x} [(1 + \nu_{xy}) \cos^2 \phi + (\nu_{xz} - \nu_{xy})] \right. \\ &\quad + \frac{\sigma_{yy}}{E_y} [(1 + \nu_{yx}) \sin^2 \phi + (\nu_{yz} - \nu_{yx})] \\ &\quad - \frac{\sigma_{zz}}{E_z} (1 + \nu_{zy} \sin^2 \phi + \nu_{zx} \cos^2 \phi) \\ &\quad + \left. \frac{\tau_{xy}}{2G_{xy}} \sin 2\phi \right\} + \sin 2\psi \left[\frac{\tau_{yz}}{2G_{yz}} \sin \phi \right. \\ &\quad \left. + \frac{\tau_{xz}}{2G_{xz}} \cos \phi \right] - \left(\frac{\nu_{xz}}{E_x} \sigma_{xx} + \frac{\nu_{yz}}{E_y} \sigma_{yy} - \frac{\sigma_{zz}}{E_z} \right), \end{aligned} \quad (10)$$

where ν_{xy} , ν_{xz} , ν_{yx} , ν_{yz} , ν_{zy} , and ν_{zx} are the Poisson coefficients; E_x , E_y , and E_z are the Young's moduli; and G_{xz} , G_{xy} , and G_{yz} are the shear's moduli in the x , y , and z directions, respectively. The last expressions represent the new

$$M_w = \begin{pmatrix} \cos^2 \psi \cos^2 \phi & \sin^2 \psi & -\cos \psi \sin \phi \sin \psi & -\cos \psi \cos \phi \sin \psi & \cos^2 \psi \cos \phi \sin \phi & -\sin \phi \cos \phi \\ \sin^2 \phi & \cos^2 \phi & 0 & 0 & 0 & -\sin \phi \cos \phi \\ \sin^2 \psi \cos^2 \phi & \sin^2 \psi \sin^2 \phi & \cos \psi \sin \phi \sin \psi & \cos \psi \cos \phi \sin \psi & -\cos \psi \sin \phi & \sin^2 \psi \cos \phi \sin \phi \\ -2 \sin \phi \sin \psi \cos \phi & 2 \sin \phi \sin \psi \cos \phi & 0 & \cos \psi \cos \phi & -\cos \psi \sin \phi & -\sin^2 \psi \sin \phi \\ 2 \cos \psi \cos^2 \phi \sin \psi & 2 \cos \psi \sin^2 \phi \sin \psi & -2 \sin \psi \cos \psi & \cos^2 \psi \sin \phi - \sin^2 \psi \sin \phi & \cos^2 \psi \cos \phi - \sin^2 \psi \cos \phi & 2 \cos \psi \cos \phi \sin \psi \sin \phi \\ -2 \cos \psi \cos \phi \sin \phi & 2 \cos \psi \cos \phi \sin \phi & 0 & -\sin \psi \cos \phi & \sin \psi \sin \phi & \cos \psi \cos^2 \phi - \cos \psi \sin^2 \phi \end{pmatrix}$$

theoretical model for analysis triaxial stress in orthotropic materials considering the shear stress. Here the superficial tension was considered, therefore $\sigma_{zz} = 0$, then putting this in Eq. (10), we obtain the following state equation of biaxial stress.

$$\begin{aligned} \varepsilon_{z'z'} = & \sin^2 \psi \left\{ \frac{\sigma_{xx}}{E_x} [(1 + \nu_{xy}) \cos^2 \phi + (\nu_{xz} - \nu_{xy})] \right. \\ & + \frac{\sigma_{yy}}{E_y} [(1 + \nu_{yx}) \sin^2 \phi + (\nu_{yz} - \nu_{yx})] \\ & \left. + \frac{\tau_{xy}}{2G_{xy}} \sin 2\phi \right\} + \sin 2\psi \left[\frac{\tau_{yz}}{2G_{yz}} \sin \phi + \frac{\tau_{xz}}{2G_{xz}} \cos \phi \right] \\ & - \left(\frac{\nu_{xz}}{E_x} \sigma_{xx} + \frac{\nu_{yz}}{E_y} \sigma_{yy} \right). \end{aligned} \quad (11)$$

This equation is the key equation used in the proposed model for the biaxial stress state. It's easy to see that the Eqs. (10) and (11) fall in Eqs. (29) and (32) of our previous model by making the assumption of negligible shear stress.

4. Analysis of consistency with experimental results for the biaxial stress state

In order to validate the new model in terms of experimental consistency, was used some useful reported experimental data from the work of Faurie *et al.*, [27]. In this work, the authors using Au thin films produced by physical vapor deposition, with a total thickness about 700 ± 10 nm.

The adopted procedure was apply these data into the new proposal model to obtain the elastic constants considering the shear stress, which was compared with those reported by Faurie *et al.*, [27,29] and our previous paper [1]. Considering the transversely isotropic anisotropy of the thin film under study, we have the conditions [22]:

$$\nu_{xz} = \nu_{yz}, \quad E_x = E_y = E, \quad \nu_{xy} = \nu_{yx}. \quad (12)$$

We emphasize that the use of biaxial stress does not allow the determination of the elastic constant E_z , furthermore, $E_z =$ undetermined for a biaxial state.

According to Faurie *et al.*, [27], the x-ray measurements were carried out in the longitudinal ($\phi = 0^\circ$) and perpendicular ($\phi = 90^\circ$) directions to the stress direction. Due to this,

the first stage of the experimental data analysis procedure begins by rewriting the expression of the model proposed in the Eq. (11) for $\phi = 0^\circ$, that is,

$$\varepsilon_{0,\psi} = A_0 \sin^2 \psi + B_0 \sin 2\psi + C_0, \quad (13)$$

where the A_0 , B_0 and C_0 coefficients have the following expressions:

$$A_0 = \frac{\sigma_{xx}}{E_x} (1 + \nu_{xz}) + \frac{\sigma_{yy}}{E_y} (\nu_{xz} - \nu_{xy}), \quad (14)$$

$$B_0 = \frac{\tau_{xz}}{2G_{xz}}, \quad (15)$$

$$C_0 = - \left(\frac{\nu_{xz}}{E_x} \sigma_{xx} + \frac{\nu_{yz}}{E_y} \sigma_{yy} \right). \quad (16)$$

Figure 1 shows a very good non-linear fitting of $\varepsilon_{0^\circ,\psi}$ experimental data. Here we show the analysis of the preliminary experimental results of the application of the proposed new theoretical model, for analysis of thin films in states with biaxial stresses. The Figs. 1 and 2, represents the experimental data with a load applied to the sample with stresses in the x and y directions. For the values of $\phi = 0^\circ$ and 90° the strain average according to the theoretical Eq. (11) in our new model was used, to obtain the elastic constants.

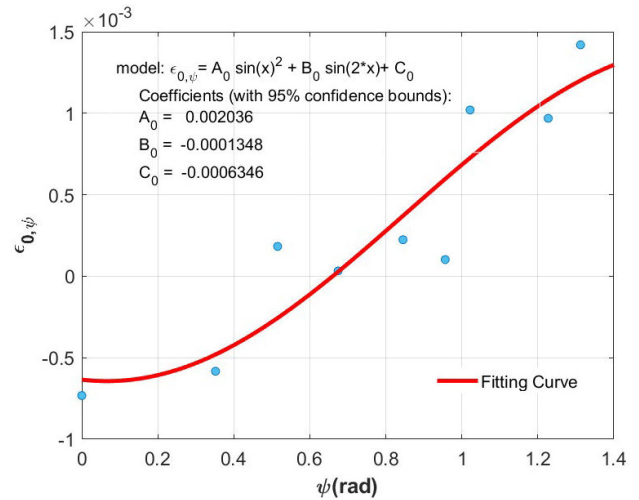


FIGURE 1. The non-linear fit behavior of experimental data $\varepsilon_{0^\circ,\psi}$ vs ψ for longitudinal directions ($\phi = 0^\circ$).

TABLE I. Performance comparison of elastic constants.

| Model | E (GPa) | | ν | | G (GPa) |
|---------------------------|------------|--------------------|--------------------|--------------------|-----------------|
| Faurie <i>et al.</i> [27] | $E = 75.7$ | E_z undetermined | $\nu = 0.517$ | - | - |
| Santos <i>et al.</i> [1] | $E = 74.1$ | E_z undetermined | $\nu_{xy} = 0.551$ | $\nu_{xz} = 0.311$ | - |
| Faurie <i>et al.</i> [29] | $E = 91$ | $E_z = 117$ | $\nu_{xy} = 0.53$ | $\nu_{xz} = 0.30$ | $G_{xz} = 0.02$ |
| Ours | $E = 78.6$ | E_z undetermined | $\nu_{xy} = 0.59$ | $\nu_{xz} = 0.34$ | $G_{xz} = 0.3$ |

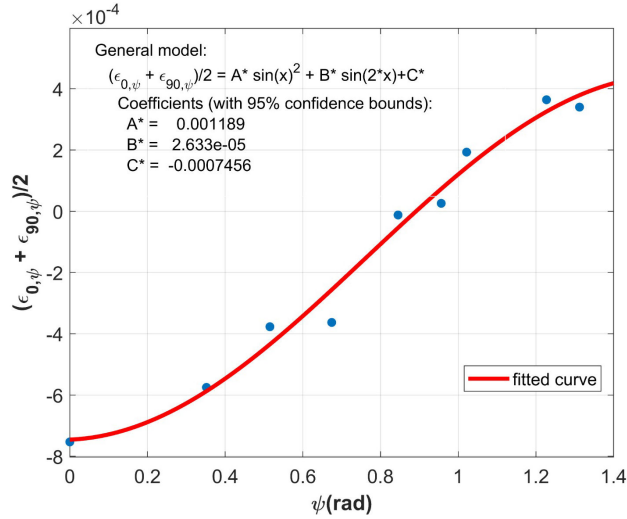


FIGURE 2. Au thin-film mean strain for $\phi = 0^\circ, 90^\circ$ versus ψ .

In similar way, we can rewrite the Eq. (11) for values of $\phi = 90^\circ$, that is,

$$\epsilon_{90,\psi} = A_{90} \sin^2 \psi + B_{90} \sin 2\psi + C_{90}, \quad (17)$$

where the A_{90} , B_{90} and C_{90} coefficients have the following expressions,

$$A_{90} = \frac{\sigma_{xx}}{E_x}(\nu_{xz} - \nu_{xy}) + \frac{\sigma_{yy}}{E_y}(1 + \nu_{yz}), \quad (18)$$

$$B_{90} = \frac{\tau_{yz}}{2G_{xz}}, \quad (19)$$

$$C_{90} = -\left(\frac{\nu_{xz}}{E_x}\sigma_{xx} + \frac{\nu_{yz}}{E_y}\sigma_{yy}\right). \quad (20)$$

Finally, the last step we did was to found the average between the Eqs. (13) and (17), obtained the following expression,

$$\frac{1}{2}(\epsilon_{0,\psi} + \epsilon_{90,\psi}) = A^* \sin^2 \psi + B^* \sin 2\psi + C^*, \quad (21)$$

where the A^* , B^* and C^* coefficients can be defined as,

$$A^* = \frac{1}{2E}(1 + 2\nu_{xz} - \nu_{xy}) + (\sigma_{xx} + \sigma_{yy}), \quad (22)$$

$$B^* = \frac{\tau_{xz} + \tau_{yz}}{4G_{xz}}, \quad (23)$$

$$C^* = -\frac{\nu_{xz}}{2E}(\sigma_{xx} + \sigma_{yy}). \quad (24)$$

Now we used the followings values, from to Faurie *et al.*, [27], $\sigma_{yy} = 135$ MPa, $\sigma_{zz} = 37$ MPa. The shear stress values was $\tau_{xz} = 0.01575$ MPa and $\tau_{yz} = 0.00185$ MPa. In addition to these data, the nonlinear fit coefficients from our proposed model, and shown in Fig. 2, were used to determine, through Eqs. (22) - (24), the elastic constants presented in Table I.

Also, in Table I we show a performance comparison of the elastic constants obtained by our proposed model with those obtained by Santos *et al.* [1] and Faurie *et al.* [27]. We observe that the elastic constants obtained using our model are consistent in terms of magnitude with the coefficients obtained by Faurie *et al.* [29], except the constant related with Shear modulus G_{xz} . This difference could be explained, because in our proposed model is considered the shear components of the stress tensor, in comparison with other works that did not do that. These experimental results demonstrate the consistency of our model for analysis of Biaxial and triaxial stress in orthotropic materials considering the Shear Stress.

Acknowledgment

The authors thanks Miss Yaniuska Leyva for the grammatical review of the text.

Conflict of interest declaration

The authors declare that there are no conflicts of interest in this work. Also, the authors declare that they have no affiliations with or involvement in any organization or entity with any financial interest in the subject matter or materials discussed in this manuscript.

Data availability statement

All data that support the findings of this study were taken from the references cited in the article.

1. E. M. Santos *et al.*, Model for Analysis of Biaxial and Triaxial Stresses by X-ray Diffraction Assuming Orthotropic, *Jpn. J. Appl. Phys.*, **49** (2010) 056601, <https://dx.doi.org/10.1143/JJAP.49.056601>.
2. J. Zaplotnik, J. Pišljak, M. Škarabot and M. Ravnik, Neural networks determination of material elastic constants and structures in nematic complex fluids, *Sci Rep.*, **13** (2023) 6028, <https://doi.org/10.1038/s41598-023-33134-x>.
3. H. Fukuda, A. Nagakubo and H. Ogi, Elastic constant

of dielectric nano-thin films using three-layer resonance studied by picosecond ultrasonics, *Jpn. J. Appl. Phys.* **60** (2021) SDDA05, <https://dx.doi.org/10.35848/1347-4065/abec5a>.

4. H. S. Cho, H. A. Kim, D. W. Seo and S. C. Jeoung, Poisson's ratio measurement through engraving the grid pattern inside poly(dimethylsiloxane) by ultrafast laser *Jpn. J. Appl. Phys.* **60** (2021) 101004, <https://dx.doi.org/10.35848/1347-4065/ac2424>.

5. I. Takahashi, N. Usami, K. Kutsukake, K. Morishita and K. Nakajima, Computational Investigation of Relationship between Shear Stress and Multicrystalline Structure in Silicon, *Jpn. J. Appl. Phys.* **49** (2010) 04DP01, <https://dx.doi.org/10.1143/JJAP.49.04DP01>.
6. Y. Lou, L. Chen, T. Clausmeyer, A. E. Tekkaya and J. W. Yoon, Modeling of ductile fracture from shear to balanced biaxial tension for sheet metals, *Int. J. Solids Struct.* **112** (2017) 169-184, <https://doi.org/10.1016/j.ijsolstr.2016.11.034>.
7. D. J. O'Shea, M. M. Attard and D. C. Kellermann, *Int. J. Solids Struct.* **129** (2019) 1-20, <https://dx.doi.org/10.1016/j.ijsolstr.2018.07.013>.
8. H. Gang and H. G. Kwak, A strain rate dependent orthotropic concrete material model, *Int. J. Impact Eng.* **103** (2017) 211, <https://dx.doi.org/10.1016/j.ijimpeng.2017.01.027>.
9. A. V. Melnik, X. Luo and R. W. Ogden, A para-universal relation for orthotropic materials, *Mech. Res. Commun.* **97** (2019) 46, <https://dx.doi.org/10.1016/j.mechrescom.2019.04.006>.
10. J. Zhou, J. Pan, L. Zhang, J. Zhao and Z. Li, Experimental study on mechanical behavior of high-strength high-performance concrete under biaxial loading, *Constr. Build. Mater.* **258** (2020) 119681, <https://doi.org/10.1016/j.conbuildmat.2020.119681>.
11. N. Park, T. B. Stoughton and J. W. Yoon, A new approach for fracture prediction considering general anisotropy of metal sheets, *Int. J. Plast.* **124** (2020) 199-681, <https://doi.org/10.1016/j.ijplas.2019.08.011>.
12. A. Mani, P. Aubert, F. Mercier, H. Khodja, C. Berthier and P. Houdy, Effects of residual stress on the mechanical and structural properties of TiC thin films grown by RF sputtering, *Surf. Coat. Technol.* **194** (2005) 190-195, <https://doi.org/10.1016/j.surfcoat.2004.06.017>.
13. C. Minas and L. Salasoo, Three-dimensional thermal stresses in a superconducting coil assembly, *IEEE Trans. Magn.* **27** (1991) 2381, <https://doi.org/10.1109/20.133697>.
14. X. Zhang, A. Misra, H. Wang, A. L. Lima, M. F. Hundley and R. G. Hoagland, Effects of deposition parameters on residual stresses, hardness and electrical resistivity of nanoscale twinned 330 stainless steel thin films, *J. Appl. Phys.* **97** 94302, <https://doi.org/10.1063/1.1883724>.
15. P. S. Prév y and J. T. Cammett, The influence of surface enhancement by low plasticity burnishing on the corrosion fatigue performance of AA7075-T6 *Int. J. Fatigue.* **26** (2004) 975-982, <https://doi.org/10.1016/j.ijfatigue.2004.01.010>.
16. E. C. Oliver, T. Mori, M. R. Daymond and P. J. Withers, Orientation dependence of martensite variants during loading of Fe-Pd shape memory alloy, *Scripta Mater.* **53** (2005) 609-612, <https://doi.org/10.1016/j.scriptamat.2005.04.021>.
17. P. S. Prév y, M. J. Shepard and P. R. Smith, The Effect of Low Plasticity Burnishing (LPB) on the HCF Performance and FOD Resistance of Ti-6Al-4V, *Proc. 6th National Turbine Engine HCF Conference* (2011) March 5-8, Jacksonville, FL
18. Y. D. Wang, R. L. Peng, X. L. Wang and R. L. McGreevy, High anisotropy of orientation dependent residual stress in austenite of cold rolled stainless steel, *Acta Mater.* **41** (1999) 995-1000, [https://doi.org/10.1016/S1359-6462\(99\)00248-1](https://doi.org/10.1016/S1359-6462(99)00248-1).
19. M. E. Fitzpatrick and A. Lodini, Analysis of Residual Stress by Diffraction Using Neutron and Synchrotron Radiation, (Taylor & Francis, London) (1st ed.). CRC Press.(2003) p.78, <https://doi.org/10.1201/9780203608999>.
20. H. R. Wenk and P. V. Houtte, Texture and anisotropy, *Rep. Prog. Phys.* **67** (2004) 1367-1428, <https://doi.org/10.1088/0034-4885/67/8/r02>.
21. T. Roland, D. Reirant, K. Lu and J. Lu, Fatigue life improvement through surface nanostructuring of stainless steel by means of surface mechanical attrition treatment, *Scrip. Mater.* **54** (2006) 1949-1954, <https://doi.org/10.1016/j.scriptamat.2006.01.049>.
22. B. M. Lempriere, Poisson's ratio in orthotropic materials, *AIAA J.* **6** (1968) 2226-2227, <https://doi.org/10.2514/3.4974>.
23. B. R. Lake, F. J. Appl and C. W. Bert 1970 An investigation of the hole-drilling technique for measuring planar residual stress in rectangularly orthotropic materials *Exp. Mech.* **10** (1970) 233-239, <https://doi.org/10.1007/BF02324095>.
24. G. S. Schajer, Advances in Hole-Drilling Residual Stress Measurements, *Exp. Mech.* **50** (2010) 159-168, <https://doi.org/10.1007/s11340-009-9228-7>.
25. B. M. Clemens and J. A. Bain, Stress Determination in Textured Thin Films Using X-Ray Diffraction *MRS Bull.* **17** (1992) 46-51, <https://doi.org/10.1557/S0883769400041658>.
26. D. Faurie, D. O. Renault, E. L. Bourhis, P. Villain, Ph. Goudeau and F. Badawi, Measurement of thin film elastic constants by X-ray diffraction, *Thin Solid Films* **469-470** (2004) 201, <https://doi.org/10.1016/j.tsf.2004.08.097>.
27. D. Faurie, D. O. Renault, E. L. Bourhis and Ph. Goudeau, Determination of elastic constants of a fiber-textured gold film by combining synchrotron x-ray diffraction and in situ tensile testing, *J. Appl. Phys.* **98** (2005) 093511, <https://doi.org/10.1063/1.2126154>.
28. N. T. Mascia, Concerning the elastic orthotropic model applied to wood elastic properties *Maderas: Cienc. Technol.* **5** (2003) 3-11, <https://doi.org/10.4067/S0718-221X2003000100001>.
29. D. Faurie and P. Djemia and E. Le Bourhis and P.-O. Renault and Y. Roussign  and S.M. Ch rif and R. Brenner and O. Castelnau and G. Patriarche and Ph. Goudeau, Elastic anisotropy of polycrystalline Au films: Modeling and respective contributions of X-ray diffraction, nanoindentation and Brillouin light scattering, *Acta Mater.* **58** (2010) 4998-5008, <https://doi.org/10.1016/j.actamat.2010.05.034>.
30. B. D. Annin and N. I. Ostrosablin, Anisotropy of elastic properties of materials, *J. Appl. Mech. Tech. Phys.* **49** (2008) 998-1914, <https://doi.org/10.1007/s10808-008-0124-1>.
31. L. Bos *et al.*, Classes of Anisotropic Media: A Tutorial, *Stud. Geophys. Geod.* **48** (2004) 265-287, <https://doi.org/10.1023/B:SGEG.0000015596.68104.31>.